

Swirl Acceleration in a Quasi-Steady MPD Thruster by Applied Magnetic Nozzle

IEPC-2005-54

*Presented at the 29th International Electric Propulsion Conference, Princeton University,
October 31 – November 4, 2005*

Yoichi Kagaya* and Hirokazu Tahara.†
Osaka University, Toyonaka, Osaka, 560-8531, JAPAN

Abstract: Thrust improvement has been studied by applying a divergent magnetic nozzle in a quasi-steady MPD thruster for H₂ of 0.8g/s, N₂ of 2.7g/s and Ar of 3.1g/s, in 3kA-10kA, and with applied-field up to 0.45 Tesla at the nozzle throat. Azimuthal motion of the plasma by $\mathbf{J} \times \mathbf{B}$ stabilized the high current discharge and affected the swirl acceleration in the plasma expansion. The thrust enhancements of 70 % for hydrogen and of 50 % for nitrogen and argon were obtained respectively, and were attributed to the arc current and applied-field intensity. Overrunning the optimum current condition with an increase in arc current, the swirl acceleration is reduced and does not work so remarkably to increase the thrust, caused by diverging of the swirl acceleration region to the downstream where the axial magnetic intensity is diffused and lower. Rotational frozen loss is increased with increasing applied-field intensity in the swirl acceleration. The plasma rotational motions and swirl expansion behavior have been clarified by use of high speed video camera technique. And also, the retrograde motion of the cathode spots, contrary to the Ampere rule, was observed.

Nomenclature

B_{self}	=	self-induced magnetic field caused by arc current
F_{self}	=	thrust with self-field, or thrust in normal operation
F_{swirl}	=	thrust with swirl acceleration, or thrust in applied-field operation
I_d, J	=	arc discharge current
P	=	kinetic energy of azimuthal rotational motion
R_a, R_c	=	anode radius and cathode radius
Tr	=	torque caused by azimuthal acceleration
ζ	=	configuration factor of the electromagnetic acceleration caused by the self-field
η	=	thrust enhanced ratio with applied magnetic nozzle
ξ	=	conversion efficiency of the swirl acceleration
ω_L	=	angular velocity of the plasma at the nozzle throat

* Research Engineer, Graduate school of Engineering Science, kagaya@me.es.osaka-u.ac.jp

† Associate Professor, Graduate school of Engineering Science, tahara@me.es.osaka-u.ac.jp

I. Introduction

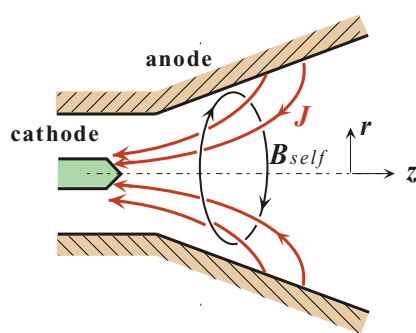
A quasi-steady MPD(MagnetoPlasmaDynamic) thruster is a electromagnetic plasma acceleration device, and applicable to a space propulsion device for reducing mission terms in future space explorations, or to use as a practical high speed plasma source for material processing or reactive coating¹. In a MPD thruster, electromagnetic plasma acceleration depends on I_d^2 , and high thrust performance is achieved by increasing of the operational arc current I_d . High current operation more than kilo amperes class is indispensable to obtain a great performance of practical use in the future applications. However, a critical condition, defined with Alfvén's critical ionization and an electromagnetic acceleration², restricts to increase the operational current within the critical current. An unstable arc discharge and vigorous erosion of the cathode and the anode break out in the excessive current operations over the critical current. Therefore, to enhance the exhaust plasma speed and to improve the thruster performance of a quasi-steady of MPD thruster within the critical condition, the effects of applying the magnetic nozzle have been investigated. The diverging magnetic nozzle up to 0.45 Tesla was applied into the arc discharge section. Thrust performance and discharge characteristics were measured to discuss the effect of the applying magnetic nozzle. Azimuthal rotational motion of the discharged plasma was observed by use of high speed video camera technique. It has been clarified that the rotational motion and swirl expansion, that is, swirl acceleration of the plasma mainly contribute to the improvement of the thrust performance with applying magnetic muzzle.

II. Swirl acceleration

Electromagnetic acceleration mechanism in a self-induced MPD thruster has been presented by Jahn³ as shown in Fig.1. The electromagnetic thrust is given by the well-known formula in Eq.1, and increase with an increase in squared arc current as I_d^2 . In many experimental studies of the self-field MPD thruster, obtainable thruster performance deviate from this formula with arc current due to a loss in the momentum exchange with drift motion of carrier particles as the electron and ion, and the thrust becomes lower than the predicted values in high current operation. The operational current should, therefore, be boosted up to near the critical condition, which defined with Alfvén's electromagnetic acceleration, in order to realize a practical propulsion device.

$$F_{\text{self}} = \frac{\mu_0 I_d^2}{4\pi} \left(\ln \frac{R_a}{R_c} + \zeta \right) \quad (1)$$

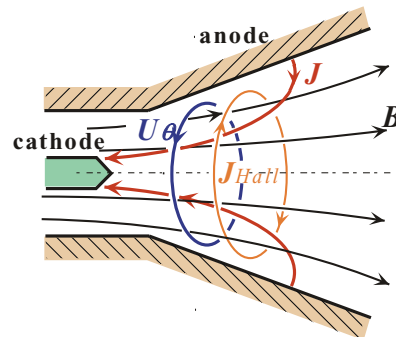
On the other hand, two electromagnetic acceleration mechanisms are expected in the applied-field MPD thruster as shown in Fig.2. Acceleration force due to $\mathbf{J}_{\text{arc}} \times \mathbf{B}_{\text{nozzle}}$ affects azimuthally and rotates the discharged plasma flow. The rotational plasma energy at the nozzle throat is converted to the axial kinetic energy with spiral expansion in the divergent section of the nozzle.



Blowing : $\mathbf{J} \times \mathbf{B}_{\text{self}}$

Pumping : $\mathbf{J} \times \mathbf{B}_{\text{self}}$

Figure 1. Plasma acceleration in self-field MPD thruster.



Swirl (∇B) : $\mathbf{J}_{\text{arc}} \times \mathbf{B}_{\text{nozzle}}$

Hall Effect : $\mathbf{J}_{\text{Hall}} \times \mathbf{B}_{\text{nozzle}}$

Figure 2. Plasma acceleration in applied field MPD thruster.

Another acceleration process with an applied magnetic nozzle is caused by the electromagnetic force $\mathbf{J}_\theta \times \mathbf{B}_{nozzle}$. Azimuthal current \mathbf{J}_θ comprises both of Hall current \mathbf{J}_{Hall} by $\mathbf{E} \times \mathbf{B}$ drift of ion and electron, and the negligibly small diamagnetic current by the pressure gradient perpendicular to the magnetic field. The body force produced by \mathbf{J}_θ , almost Hall current, affects directly in axial direction as thrust. Hall current \mathbf{J}_{Hall} is produced by dragging of azimuthal drift between electrons and ions. In the rotational motion of the discharged plasma, electron cannot outrun ion in azimuthal direction because the charge separation produce a local field to pull back the electron. Because the ion drifts in the same direction of the electron, the ion motion tends to reduce the azimuthal current. With applying the strong magnetic nozzle, the azimuthal velocity of ion comes up with the rotational velocity of electron, and Hall current becomes negligible. Therefore, swirl acceleration is dominant process compared with Hall acceleration in the MPD thruster with applied magnetic nozzle. The azimuthal Lorentz force is produced by the interaction of $\mathbf{J}_{arc} \times \mathbf{B}_{nozzle}$, and the discharged plasma is rotated in the nozzle throat. When azimuthal acceleration region confined in straight section of the nozzle throat and the plasma rotates as a solid body with uniform density, the applied torque Tr of the plasma is related with the effective anode radius and cathode radius⁴ in Eq. 2.

$$Tr = \int \frac{\partial(i\omega)}{\partial t} u_z dz = \iint r \times (J \times B) dr dz = \frac{1}{2} I_d B_z (R_a^2 - R_c^2) \quad (2)$$

Here, B and I_d are the magnetic field and the arc current, and R_a , R_c are the anode and cathode radius. From the relationship of the angular momentum and the torque of the plasma at the nozzle throat, the angular velocity of the plasma, ω_L , and the time rate of kinetic energy of the azimuthal acceleration P , are as follows and dependent on the propellant mass rate.

$$\omega_L = \frac{B I_d}{\dot{m}} \frac{R_a^2 - R_c^2}{R_a^2 + R_c^2} \quad (3)$$

$$P = u \frac{1}{2} i \omega_L^2 = \frac{C}{4} \frac{(B I_d \Delta R)^2}{\dot{m}} \quad (4)$$

Here, i is the moment of inertia of the rotating plasma at the straight throat section of the nozzle anode, and $\Delta R = (R_a - R_c)$, $C = 1 + (2R_a/R_c) / [1 + (R_a/R_c)^2]$, respectively. When all of azimuthal kinetic energy in the plasma is completely converted into axial energy in the swirl expansion at the divergent nozzle, maximum thrust F_{swirl} is given as upper limit of the swirl acceleration.

$$F_{swirl} = \sqrt{\frac{C}{2}} B I_d \Delta R \quad (5)$$

III. A quasi-steady MPD thruster with applied magnetic nozzle

The quasi-steady MPD thruster (MK-II-N) was operated in a vacuum chamber. The back pressure was kept to 1×10^{-3} Pa in firing for the thrust measurement. The experimental system consists of as follows; PFN-1 is primary pulse power supply and operated with a quasi-steady rectangular current pulse up to 10 kA for duration time of 0.6 ms. PFN-2 is exclusive power supply to drive the magnetic pulse coil to apply the magnetic nozzle field up to 0.5 Tesla at the cathode position. Two fast-acting valves (FAV) are used to inject propellant gas pulse into the thruster synchronized with arc trigger. Propellant mass flow rate are provided from the equivalent critical value of arc current of 5 kA, 10 kA and 15 kA for hydrogen, nitrogen and argon, respectively. All of the experimental system is controlled with an appropriate delayed trigger commands by the operational control unit, and time sequence of the arc discharge is strictly controlled. The

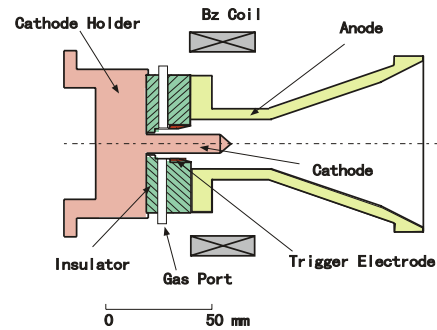


Figure 3. Cross sectional view of a MPD arc jet with applied magnetic nozzle.

MPD thruster has straight-divergent cylindrical anode, the exit diameter of 89 mm and a half angle of 20 degree in the divergent part as shown in Fig.3. In generally, such a pulsed magnetic nozzle induces an azimuthal eddy current on the anode surface and causes a self-distortion of the applied magnetic nozzle configuration. In order to avoid the distortion of the magnetic nozzle, the anode is axially silted to cut an azimuthal eddy current loop. A cylindrical cathode, made of 2 % thoriated tungsten, is 18 mm long and 9.5 mm in diameter at the discharge section. The pulse coil of the magnetic nozzle has an in-diameter of 100 mm and 50 mm long, and pulse current is supplied from PFN-2 by use of a semiconductor switch (CR250J-24) to synchronize with other thruster driver units, and the applied field of the magnetic nozzle is provided quasi-steadily in the discharge section during arc discharge. The magnetic nozzle profile is shown in Fig. 4(a), which is drawn by use of iron powder. Figure 4(b) and 4(c) show the axial and radial direction profiles of axial component B_z of the applied magnetic fields by the ratio to B_{z0} at the cathode tip position or at axial position of anode exit. The magnetic field is measured by a magnetic probe (BH-203 F.W.Bell). The magnetic field line of the nozzle is along the solid-nozzle wall and the maximum point of axial gradient, $\partial B / \partial z$, is at the halfway region of the anode discharge section (45 mm from the cathode tip).

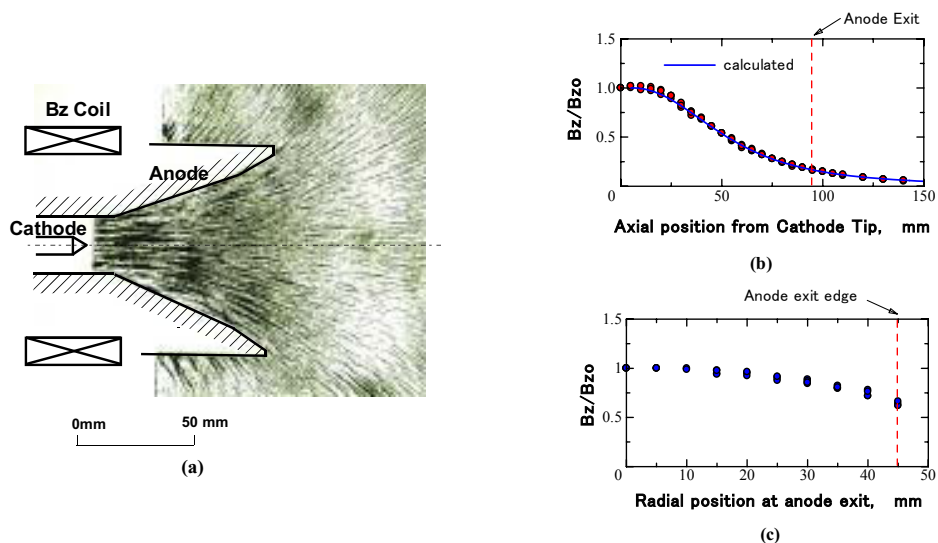


Figure 4. Profiles of applied axial magnetic nozzle.

The thrust impulse is measured by pendulum method⁵, and previously calibrated by known impulse with steel ball impacts. Faked force, due to interaction force caused by current loop on the thruster power cable and the coil power cable, is estimated and subtracted in the thrust calibration. This electromagnetic faked forces are evaluated by short-circuit at anode and cathode terminals. In this study, the faked force is suppressed negligibly compared with true thrust impulse by use of a peculiar coaxial cable. In other hand, high speed video camera (FASTCAM-APX RS, Photron) of which time resolution of 25×10^4 fps., is employed to clarify the plasma flow profiles of swirl expansion when the magnetic nozzle is applied.

IV. Arc performance and thrust improvement

The azimuthal kinetic energy is obtained from work made by the azimuthal Lorentz force due to applying the strong magnetic nozzle at the anode nozzle throat, and almost all the plasma particles are diffused with the spiral motion and diverged from anode exit to the downstream. The azimuthal rotational motion and spiral expansion of the discharged plasma have been observed to investigate the swirl acceleration mechanism by use of high speed video camera, and axial views of the plasma swirl motion have been taken from the downstream of the anode exit. The effect of the magnetic nozzle is shown in 0.4 Tesla of the applied-field at the nozzle throat in Fig.5 and Fig.6. In Fig. 5(a) without applied-field, the plasma plume is directly diffused to downstream, and the cathode jet is found in the discharged plasma plume, and the cathode tip is invisible in the plasma plume in the axial view of Fig.6(a).

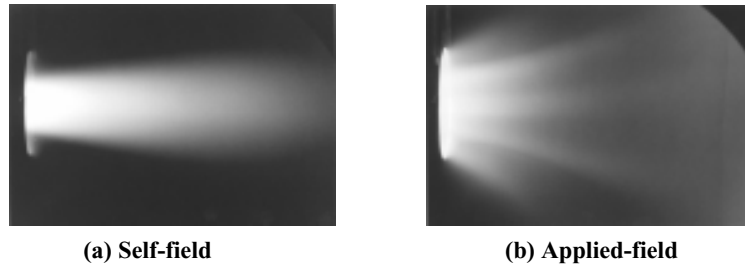


Figure 5. Side view of plume expansion with a magnetic nozzle, (N_2 , 2.7 g/s, 6 kA).

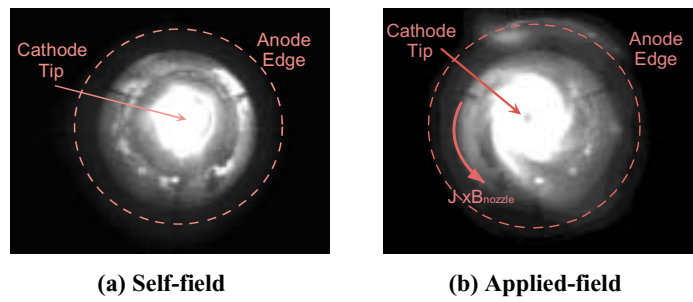


Figure 6. Axial view of swirl motion with a magnetic nozzle, (N_2 , 2.7 g/s, 6 kA).

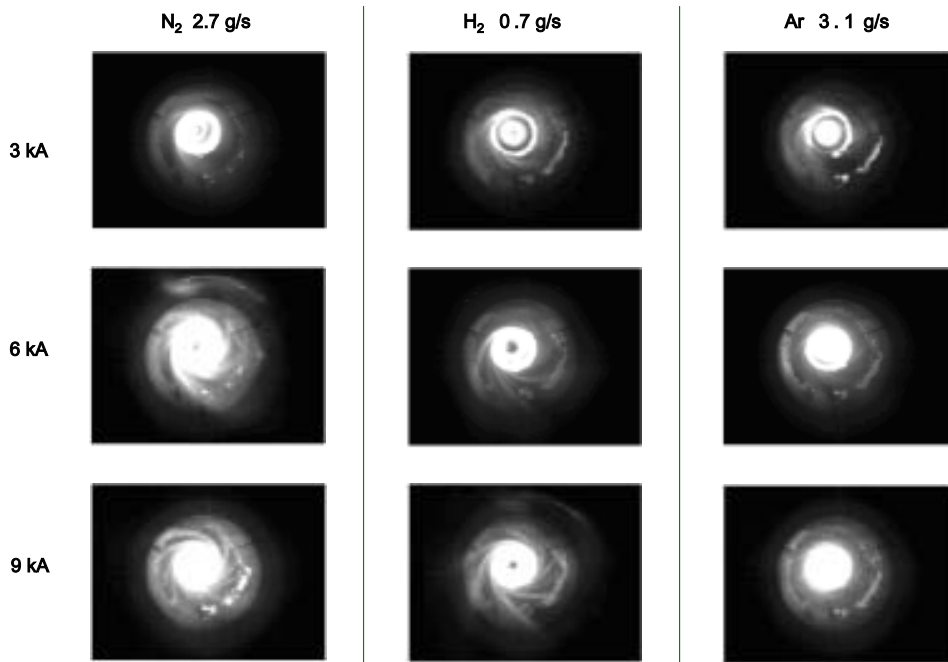


Figure 7. Swirl expansion behavior of plasma plume for N_2 , H_2 and Ar at 3kA, 6kA, and 9kA.

However, in Fig.5(b) with applied magnetic field, the plasma plume is remarkably diverged perpendicularly to the applied magnetic field, and rotated azimuthally in counterclockwise caused by Lorentz force of $\mathbf{J}_{arc} \times \mathbf{B}_{nozzle}$, and the central core of the plasma plume is diffused to radial direction with a drastic spiral motion and thereby the cathode tip appears in the rotational plasma, as shown in Fig.6(b) of the axial view. Because only the particles which have a low pitch angle of the spiral expansion can pass through the core region of the diverging nozzle, just like as in a magnetic plasma mirror, almost of the plasma particles are excluded from the core region and diffused to the divergent anode wall perpendicularly to the magnetic field, and the plasma density goes down in the central region of the discharged plasma⁶. These swirl motions of the discharged plasma have been observed, similarly for other propellants, as shown in Fig.7 with applied-field of 0.4 Tesla at the nozzle throat. With increasing of the arc current, the spiral motion extends toward the downstream and remains in the anode divergent section, which brings about an incomplete conversion of the azimuthal kinetic energy to the axial kinetic energy in the swirl acceleration. The discharged plasma behaviors of the swirl expansion are characterized by the used the propellant species and arc current, as shown in Fig.7 in 3kA. In a light gas species such as hydrogen, the spiral motion of the discharged plasma is intensified remarkably and extends toward the downstream with an increase in arc current. Angular frequency of plasma rotation at the throat section of the anode divergent nozzle was about 10 kHz for any gas species, and this value is small compared with the predicted one by Eq.(3). In addition, a retrograde motion⁷ of the cathode arc contacted points, which moves in the opposite direction contrary to the Ampere rule, has been observed. The retrograde motion is generally accepted the phenomenon caused by uneven distribution of the arc current over the whole contact area of the arc plasma with the cathode surface in a cold-cathode arc discharge. In the retrograde motion, the cathode spots move the opposite (retrograde) direction contrary to the azimuthal Lorentz force of $\mathbf{J}_{arc} \times \mathbf{B}_{nozzle}$, and the measured angular frequency of the retrograde motion was not more a few kHz for any propellant. The thrust improvement caused by the applied magnetic nozzle has been confirmed in the thrust measurement, as shown in Fig.8 for each propellant of (a) hydrogen, (b) nitrogen and (c) argon. (Self) line is plotted the theoretical thrust provided by Eq. (1), and (Self + Swirl) line indicates the ideal total thrust added with the swirl acceleration of Eq.(5) in the MPD thruster. Red solid points indicate the measured values of the total thrust with applied-field of 0.3 Tesla at the nozzle throat, and circular points show the measured thrust in the self-field. And also Blue solid points in Fig.8(a), indicate the previous experimental results of another self-field type of MPD thruster (MY-I)⁸ which has a cylindrical anode for illustrative purposes. MPD thruster (MK-II-N), as shown in Fig.3, has a divergent anode to improve the plasma acceleration in the self-field operation. Thrust improvement by the divergent nozzle anode has confirmed for other propellant species. In addition, the thrust performance has improved by applying the magnetic nozzle. With increasing the arc current, the magnetic nozzle affects to improve the thrust. And that enhancement is remarkably for light gas such as hydrogen. However, when the arc current was more increased and come up to Alfvén's critical current⁹ which in this case is about 10 kA for any propellant, the applied-field effect is reduced, and the thrust approaches one in the self field with increasing of current for any propellant species, as shown in Fig. 8. When all of the arc contacts evenly distribute on the straight section of the electrodes, the obtainable thrust with a swirl acceleration is idealized in Eq.(5), In our previous experimental study¹⁰ in the MPD thruster, it has been clarified that the current distribution of the arc discharged is extended to the downstream in the diverging section with increasing of arc current, and it has been characterized by both of propellant gas species and operational arc current. Therefore, the reduction of swirl acceleration with excessively increasing arc current is attributed to extend the arc distribution in the downstream of anode divergent section.

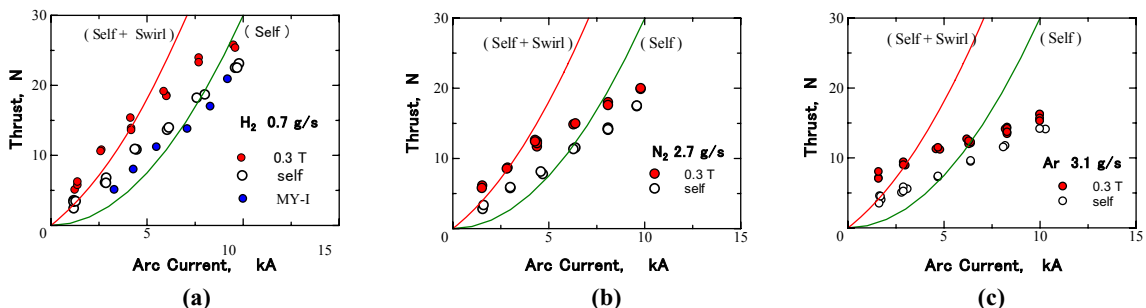


Figure 8. Thrust performance in self-field and in applied-field of 0.3 Tesla at nozzle throat.

The swirl acceleration is attributed to both of the azimuthal acceleration of the plasma and the energy conversion with axial magnetic gradient in the plasma expansion. The azimuthal Lorentz force $\mathbf{J}_{arc} \times \mathbf{B}_{nozzle}$ is closely dependent on diverging of the arc distribution and the axial magnetic field. When the arc current distribution extends to the downstream, where the applied-field is divergent as shown in Fig.4, the cross angle between the arc current direction and the applied-field line is on the decrease with extending of arc current, and the azimuthal acceleration region is diffused and shifted from the nozzle throat to the downstream with an increase in the operational arc current, as shown in Fig.7. Thus, the azimuthal kinetic energy, produced from the work made by the azimuthal acceleration, is reduced. That is, the diverging of the arc distribution affects to reduce the angular momentum caused by azimuthal Lorentz force $\mathbf{J}_{arc} \times \mathbf{B}_{nozzle}$, and also the unrecoverable frozen loss of the azimuthal rotational energy is increased in the swirl expansion with an increase in the arc current. Thereby, the thrust improvement with applied-field is dependent on both of the arc current distribution caused by the discharge conditions and the configuration of the magnetic nozzle.

Here, thrust enhanced ratio with the applied magnetic nozzle is defined as η , in Eq.(6), and the theoretical equation of η is derived from Eq.(1) of a thrust caused by electromagnetic acceleration due to the self-induced magnetic field and Eq.(5) of a thrust due to swirl acceleration with an applied magnetic nozzle. ξ means a conversion factor to an ideally swirl acceleration. ξ' is an experimental conversion factor to the swirl acceleration due to the applied magnetic field. And these ratios are attributed to both of the azimuthal acceleration efficiency for the torque obtained from the axial Lorentz force in the discharged section and the conversion efficiency of axial kinetics due to the magnetic gradient in the swirl expansion. When the arc current contacts in the straight section of the anode surface and distributes evenly over the contact area of the arc plasma, an ideal torque caused by azimuthal Lorentz force is given to the plasma, and the swirl acceleration is ideally obtained by the swirl expansion with according to a fully conservation law of magnetic moment and kinetic energy. The conversion factor of swirl acceleration ξ means the deviation of the ideal swirl acceleration, and is attributed to the efficiency of the azimuthal acceleration and a frozen loss of the swirl expansion caused by the arc distribution and the nozzle configuration. The relation of the thrust enhanced ratio η and arc current is plotted with the applied-field intensity at the nozzle throat as in Fig. 9 for $\xi=1.0$, $\xi=0.5$, and $\xi=0.3$.

$$\eta = \frac{F_{self} + \xi F_{swirl}}{F_{self}} \cong 1 + \frac{\xi' F_{swirl}}{F_{nomal}} \quad (6)$$

$$(0 \leq \xi, \xi' \leq 1)$$

The thrust enhancement caused by the applied-field is dependent on not only applied-field intensity but the operational arc current, strongly, as shown in Fig.9. And the thrust enhanced ratio η is remarkably reduced and gradually approaches to unity with an increase in arc current, and also the conversion factor ξ greatly affects the enhancement of thrust. Especially with a decrease in the conversion factor ξ , the enhancement of thrust is defected in lower current not more than the critical operation. In Fig.9, the applied magnetic nozzle remarkably affects with

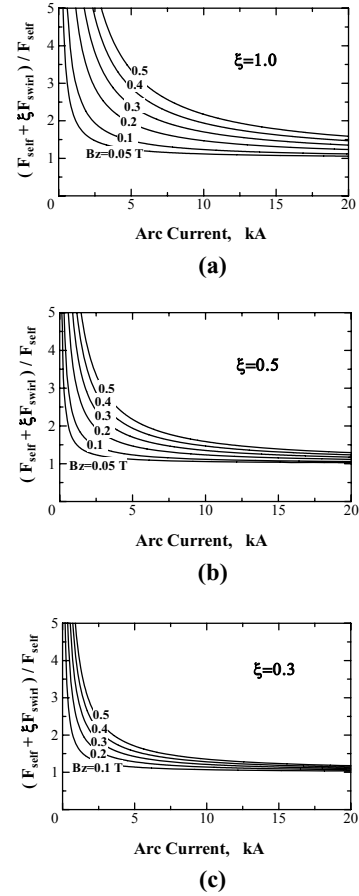


Figure 9. Ratio of the thrust in self-field to whole thrust in applied-field.

increasing of the conversion factor ξ , and the thrust of swirl acceleration is increased with an increase in applied-field intensity. An ideal swirl acceleration caused by the applied magnetic nozzle is regarded as the kinetic energy conversion from the azimuthal acceleration in the nozzle throat to axial kinetic motion caused by the completely trapped plasma particles with the conservation of the magnetic moment in the expansion of the magnetic divergent nozzle. The magnetic moment of the plasma given by the azimuthal Lorentz force is converted to the axial kinetic force by the axial gradient of the magnetic field in the diverging section of the magnetic nozzle¹¹. Energy conversion and enthalpy loss in the swirl acceleration of the plasma is remarkably attributed to Hall parameter of the plasma in the particle collision in the diverging process. Therefore the propellant species, which has a large Hall parameter is advantageous to be affected an electromagnetic acceleration, and to improve the swirl acceleration. A light gas species advantages to reduce the loss in the energy conversion process of swirl acceleration, since the plasma of a light gas species, like as hydrogen, has large Hall parameter, compared with heavy gas. Therefore, the ratio ξ is attributed to the Hall parameter and the current contacted ratio at the anode straight section, and the swirl

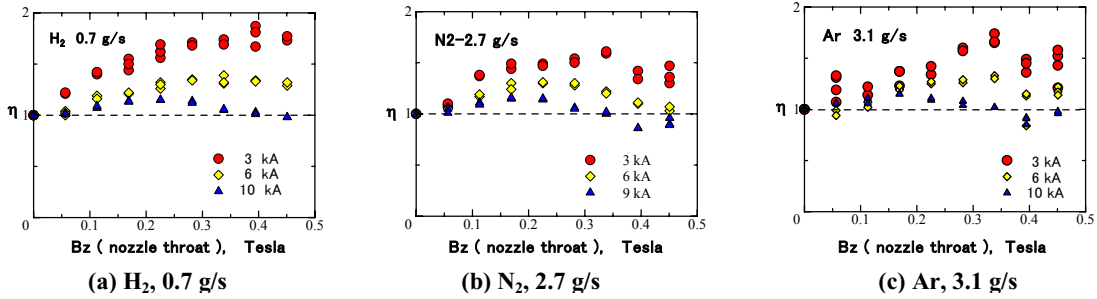


Figure 10. Thrust enhancement with swirl acceleration for B_z of nozzle throat.

acceleration is enhanced by the use of hydrogen. The results of thrust measurement are summarized with the intensity of the applied magnetic nozzle in Fig.10. Remarkable enhancement of thrust is found with increasing of applied-field in lower operational current, and with moreover increasing of the current, the thrust enhanced ratio of η levels off or comes up to maximum at a proper intensity of the magnetic nozzle with increasing of applied-field, that is, excessive applied magnetic field affects to reduce the swirl acceleration. These properties are noticeable with increasing arc current. These results can be regarded that an increase in the intensity of the applied-field improves the azimuthal acceleration in the downstream of the divergent section, but excessive increasing of the applied-field makes to leave a rotational energy component to the exhausted plasma by the incomplete swirl acceleration, and the acceleration loss is increased in the divergent section of magnetic nozzle.

The experimental energy conversion factor ξ' involves both of the azimuthal acceleration efficiency and swirl acceleration efficiency in spiral expansion of the plasma motion, and strongly dependent on applied-field as shown in Fig.11. The efficiency comes up to about 0.5 to 0.3 of the peak value at a proper intensity of applied-field for any

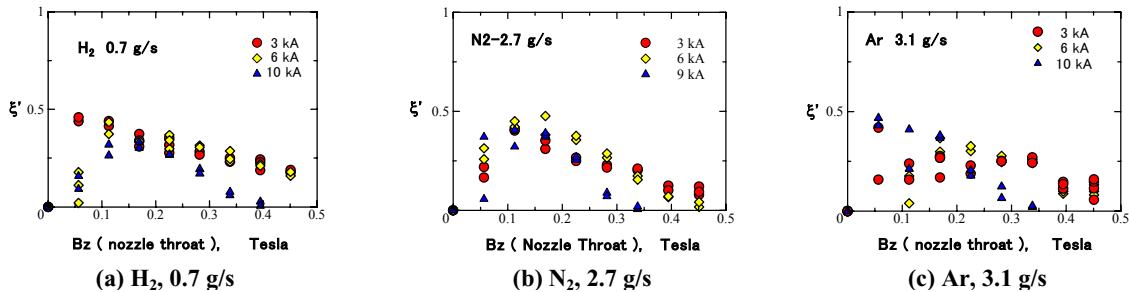


Figure 11. Conversion factor of swirl acceleration for B_z of nozzle throat.

propellant species. In addition, with increasing of the applied-field intensity, ξ' is remarkably reduced caused by increasing of frozen loss in the spiral expansion, and also with an increase in the arc current of 3 kA to 9 kA, it is reduced by reduction of the azimuthal acceleration in the nozzle throat with the diverging of arc distribution. The experimental conversion factor ξ' was 0.5 or less, and depended on both of the diverging of arc distribution on the anode surface and a configuration of magnetic nozzle.

V. Conclusions

Effects of the divergent magnetic nozzle have been investigated to improve the thrust performance in the quasi-steady MPD thruster. The swirl acceleration is one of the electromagnetic plasma phenomena caused by $\mathbf{J}_{arc} \times \mathbf{B}_{nozzle}$, and remarkably dependent on the arc operational current and the intensity of magnetic nozzle. The most effective condition to improve the thrust performance was found for several propellant species. The thrust were improved up to 50 % for nitrogen and argon, and 70 % for hydrogen. It is necessary to investigate energy conversion process from azimuthal acceleration to axial kinetic acceleration in swirl acceleration, and the anode configuration and the magnetic nozzle field should be reconsidered to recover the rotational frozen loss of the exhausted plasma jet, and to improve the swirl acceleration in high current operation near the critical condition. In addition, the reversal motion of the cathode spots, contrary to the Ampere rule, is very interesting phenomenon in the MPD thruster with applied magnetic nozzle, and the influence for the azimuthal acceleration in the nozzle throat should be hereafter clarified.

VI. References

- ¹Shibata, T., Tahara, H., Yasui, T., Kagaya, Y., and Yoshikawa, T., "Development of an Electromagnetic Acceleration Plasma Generator for Zirconia and Titanium Nitride Coatings," *Proceeding of the 26th International Propulsion Conference*, IEPC99-197, Vol.2, Kitakyushu, 1999, pp. 1153-1158.
- ²Nerheim, N. M., and Kell, A. J., "A Critical Review of the Magneto-plasma-dynamic (MPD) Thruster for Space Application," California Inst. of Technology, Jet Propulsion Lab., TR 32-1196, Pasadena, CA, Feb. 1968.
- ³Jahn, R. G., *Physics of Electric Propulsion*, McGraw-Hill, New York, 1968, Chaps.8.
- ⁴Fradkin, D. B., Blackstock, A. W., Roehling, D. J., Stratton, T. F., Williams, M. and Liewer, K. W., "Experiments Using a 25-kW Hollow Cathode Lithium Vapor MPD Arcjet," *AIAA Journal*, Vol. 8, No. 5, May 1970, pp. 886-894.
- ⁵Kagaya, Y., Tahara, H., and Yoshikawa, T., "Electrode Power Loss and Thruster Performance of a Pulsed MPD Accelerator," *Proceeding of the 26th International Propulsion Conference*, IEPC99-172, Vol.2, Kitakyushu, 1999, pp. 985-991.
- ⁶Kagaya, Y., Tahara, H., and Yoshikawa, T., "Effect of Applied Magnetic Nozzle in A Quasi-Steady MPD Thruster," *Proceeding of the 28th International Propulsion Conference* [CD-ROM] IEPC031, Vol.1, Toulouse, 2003.
- ⁷Michel G. Drouet, "The Physics of the Retrograde Motion of the Electric Arc," *Japanese Journal of Applied Physics*, Vol.20, No.6, June, 1981, 1027-1036.
- ⁸Tahara, H., Kagaya, Y. and Yoshikawa, T., "Hybrid MPD Thruster with Axial and Cusp Magnetic Fields," *Proceeding of the 20th International Propulsion Conference*, IEPC88-058, Vol.1, Garmisch-Partenkirchen, 1988, pp. 102-111.
- ⁹Malliaris, A. C., John, R. L. Garrison, R. L., and Libby, D. R., "Quasi Steady MPD Propulsion at High Power," NASA CR-111872, 1971.
- ¹⁰Tahara, H., Sasaki, M., Kagaya, Y., and Yoshikawa, T., "Thrust Performance and Acceleration Mechanisms of a Quasi-Steady Applied-Field MPD Arcjet," *Proceeding of the 21th International Propulsion Conference*, AIAA90-2554, Orlando, FL, 1990.
- ¹¹Chen, F. F., *Introduction to Plasma Physics*, Plenum Press, New York, 1974, Chap.2.